Multilevel modulation of a sensory motor circuit during *C. elegans* sleep and arousal

Julie Y. Cho[1] and **Paul W. Sternberg**[1,2]

Paul W. Sternberg: pws@caltech.edu

[1]Division of Biology and Biological Engineering, California Institute of Technology, Pasadena, California 91125

[2]Howard Hughes Medical Institute, California Institute of Technology, Pasadena, California 91125

Abstract

Sleep is characterized by behavioral quiescence, homeostasis, increased arousal threshold, and rapid reversibility. Understanding how these properties are encoded by a neuronal circuit has been difficult, and no single molecular or neuronal pathway has been shown to be responsible for the regulation of sleep. Taking advantage of the well-mapped neuronal connections of *Caenorhabditis elegans* and the sleep-like states in this animal, we demonstrate the changed properties of both sensory neurons and downstream interneurons that mediate sleep and arousal. The ASH sensory neuron displays reduced sensitivity to stimuli in the sleep-like state, and the activity of the corresponding interneurons in ASH's motor circuit becomes asynchronous. Restoration of interneuron synchrony is sufficient for arousal. The multilevel circuit depression revealed provides an elegant strategy to promote a robust decrease in arousal while allowing for rapid reversibility of the sleep state.

Keywords

Sleep; Neural Circuit; ChR2; GCaMP; Cameleon; Avoidance

Introduction

Sleep behavior is conserved and present in essentially all animal species as a lack of reactivity to sensory inputs, low activity, decreased conscious awareness, and rapid reversibility to wakefulness (Allada and Siegel, 2008; Siegel, 2001). Despite long-standing knowledge and characterization of these states, translation to a physiological or circuit definition has been difficult for many reasons. No single molecular or neuronal pathway has been shown to be responsible for the regulation of sleep, and incomplete knowledge of connections in sensory motor circuits of many studied species precludes interrogation of the flow of information that promotes sensory responses. Furthermore, the complexity and redundancy of the mammalian nervous system complicates the understanding of the flow of information. Here we use the nematode *C. elegans* to define sleep behavior in a simple sensory motor circuit.

C. elegans exhibits sleep-like behaviors during lethargus, a quiescent state during which locomotion and feeding are suppressed (Van Buskirk and Sternberg, 2007) and sensory arousal is decreased (Raizen et al., 2008). Lethargus lasts two to three hours, and like sleep it exhibits homeostasis: upon disruption or deprivation during the normal resting period, there is a period of anachronistic rebound rest (Raizen et al., 2008). During lethargus, worms exhibit delayed or decreased avoidance behavior in response to both mechanical and chemical stimuli, and this response delay is reversible upon previous stimulation of the same neuron (Raizen et al., 2008). Quiescence as measured by decreased feeding and locomotory behavior is also present in adult satiety behavior (You et al., 2008). However, the dynamics of this state were not previously studied.

Lethargus invariably occurs during development after each of the four larval stages, and the timing of lethargus corresponds to increased expression of LIN-42, homolog of circadian regulator PER (Monsalve et al., 2011). In addition, several additional conserved regulators have been identified. Anachronistic quiescence is also induced by expression of EGF (Van Buskirk and Sternberg, 2007), a function conserved in mammals (Zimmerman et al., 2008) and Drosophila (Foltenyi et al., 2007), and sensory arousal can be depressed by PKG (Raizen et al., 2008), another well-conserved signaling protein. Conservation of sleep characteristics and molecular signaling suggests that the lethargus state in *C. elegans* could prove insightful in understanding sleep regulation.

The connections of the *C. elegans* nervous system are mapped (Ward et al., 1975; White et al., 1986), and functional circuits mediating avoidance defined (Bargmann, 2006). Avoidance behaviors are mediated by mechanosensory and chemosensory neurons that activate downstream circuit components to coordinate motor neuron activity and locomotion. The ASH sensory neuron drives an avoidance circuit and promotes immediate locomotory reversal (Figure 1A). When animals are presented with ASH-specific stimuli, ASH stimulates interneurons AVA and AVD, which in turn induces backward locomotion through stimulation of excitatory cholinergic motor neurons in the ventral cord (Figure 1a) (Guo et al., 2009; Hilliard et al., 2005; Hilliard et al., 2002). Evidence of altered arousal as measured by response delay to ASH-specific stimuli suggests modulation in the avoidance circuit during sleep behavior.

Many tools exist to probe and study neural circuits in *C. elegans*. Use of known transcriptional control regions of characterized genes drive expression of genetically encoded calcium sensors and allow measurement of activity in single or multiple cells. Cameleon is a dual channel ratiometric reporter that corrects for changes in reporter expression over states, stages and time. However, Cameleon has slower dynamics because it involves energy exchange between two fluorophores, and GCaMP, a single channel reporter, has better dynamic range. Therefore, we used both reporters: cameleon controlled for state-related changes in reporter expression and GCaMP allowed measurement of smaller calcium events. Activity patterns observed can be mimicked using light-driven cation channels such as channelrhodopsin (ChR2). Similar to the calcium sensors, ChR2 is genetically encoded and expression in select cells using specific promoters as well as combinatorial approaches that allow expression only where two promoters overlap or that allow expression only in cells that are unique to one promoter in the pair. These strategies allow measurement and activation of specific components of pertinent circuits. Here we use genetically encoded calcium sensors and light-driven channels to investigate the ASH circuit during sleep and waking. We find that multiple steps in the circuit are dampened during sleep.

Results

ASH sensory neuron exhibits decreased sensory response to disparate stimuli in lethargus

The amphid sensory neuron, ASH, senses multiple aversive stimuli including mechanical stimulation at the tip of the head, and noxious chemical cues, such as copper, 1-octanol, or high osmolarity (Hilliard et al., 2005). We used a chemical stimulus to characterize ASH activity during a "sleep cycle" because it is more consistent and controllable than mechanical stimuli. We fabricated a modified version of a microfluidic olfactory chip (Chronis et al., 2007) to accommodate and immobilize fourth larval stage (L4), lethargus, and young adult animals (Figure 1B). These devices permitted temporally controlled delivery of chemical stimuli and simultaneous fluorescence imaging from the ASH. Individual animals were assayed for a 6-hour period during which they were subjected to a brief stimulus every 30 minutes. ASH response was measured during these intervals using the calcium indicator GCaMP3 (Yizhar et al., 2011). Each animal was imaged before, during and after lethargus. Chemosensory neurons use ligand-binding receptors to open ion channels (Bargmann, 2006), and ASH responds to the addition of 1mM Cu^{2+} with a robust increase of calcium concentration in the L4 stage. During lethargus, the magnitude of ASH response decreases significantly to copper or glycerol, but full responsivity is recovered upon exit from lethargus (Figure 1C, S1A).

To confirm this result and control for confounding factors such as changes in GCaMP expression and baseline calcium levels, short assays were performed using ratiometric imaging with the calcium sensor Cameleon (Yizhar et al., 2011). In these assays, animals of each stage were loaded into the device, imaged within an hour of loading for both baseline and stimulus measurements, and discarded. These short assays were consistent with the longitudinal analysis: there was significant decrease in calcium levels as measured by the peak fluorescence change in response to the chemical copper and glycerol (Figure 1D–E, S1A). Moreover, the availability of fluorescent indicator and baseline calcium concentration did not change sufficiently among behavioral states to account for the decrease in calcium levels (Figure S1B–C). Therefore, the calcium imaging data suggest that there are fewer calcium channels open, and thus the same stimulus is less able to excite the ASH sensory neuron during lethargus. This result is consistent with decreased calcium dynamics observed in the mechanosensory neuron, ALM, during lethargus (Schwarz et al., 2011). Furthermore, stimulus-evoked calcium transients were not ligand specific as evidenced by decreased response to both copper and glycerol and suggest that modulation in lethargus may affect general excitability or synaptic activity of the ASH neuron.

Basal activity of AVA is reduced in lethargus

We next examined the interneuron level in the circuit. Calcium levels in AVA oscillate and increasing levels correspond to behavioral reversals (Ben Arous et al., 2010). We observed that oscillation of AVA activity is not regular and disappears in lethargus, but reappears in the young adult animals (Figure S2A–B). Thus, we confirmed the published GCaMP3 findings in AVA with Cameleon measurements. Furthermore, the basal activity and the context in which AVA receives input from ASH changes during lethargus.

Synchrony between AVD and AVA interneurons is lost in lethargus

To assess activity across the top two layers of the circuit, we used animals expressing GCaMP3 in ASH, AVD, and AVA. To examine stimulus-driven interneuron activity, we measured response to an ASH-specific cue (1M glycerol) (Hilliard et al., 2002), which has less variable dynamics (Figure S1A). Each 60-second trial consisted of a 10s pulse of control buffer or glycerol; trials with discernable ASH responses were chosen, and

instantaneous slopes were calculated over the imaging interval to represent the magnitude of the calcium increases. In young adult animals without stimulation, the timing of the calcium increases showed no association with the pulse of control buffer and did not occur during the stimulus interval (Figure S3D). However, after a glycerol stimulus, the increase of calcium in the AVD and AVA was associated with the stimulation interval (Figure 2B–C). AVD and AVA showed both decreased responsivity during lethargus as well as a loss of coordinated calcium activity. Animals in lethargus exhibited very little activity in the AVD and AVA, and fluctuating calcium levels during the glycerol stimulus were not significantly different from the period preceding the stimulus (Figure 2B). Because the magnitude of activity is considerably smaller in lethargus compared to the young adult, we had to normalize these measurements as binary values. Positive changes in fluorescence were thus counted as individual calcium increases. There were significantly more increases during the glycerol stimulus in the young adult, but often little activity was seen in AVA during lethargus even when AVD activity was noted (Figure 2C, E).

To test for association of ASH-interneuron and AVD-AVA activity, we compared the timing of initiation and duration of the calcium transients between neuron pairs by performing cross correlation analysis between each of the neurons imaged. Comparing data for timing between of calcium events between pairs allows us to assess functional correlation between neurons. This cross correlation analysis indicates that when compared to the input ASH neuron, AVD transients exhibit a lag during lethargus whereas AVA transients do not (Figure 2D–E). This observation suggests that when awake, AVD and AVA receive signal from the ASH and exhibit simultaneous calcium transients, whereas AVD in a lethargus animal is desynchronized with AVA. We further analyzed AVD and AVA for instances of repetitive calcium transients. There was a significant decrease of coupled trains during lethargus: a majority of the traces did not show activity in both neurons, and uncoupled activity was present during lethargus (Figure 2F–G). Moreover, the number of AVA only traces did not differ significantly from the number of AVD only traces (Figure 2G), suggesting that alterations of synaptic transmission are not specific to a particular synapse.

These results indicate that coupled activity in the command interneurons occur in the awake state and may not only explain processing delay during lethargus but also suggests that synaptic transmission downstream of ASH becomes variable and differs across independent synapses. The altered efficacy of ASH-AVD and ASH-AVA synapses could be due to decreases in either presynaptic transmission or postsynaptic excitability. However, while it is possible that the ASH compartment presynaptic to AVD may vary independently from that which is presynaptic to AVA, the calcium measurements in the ASH show no indications that this is the case. In addition, synapse specific changes or lags in activity usually show a general preference for a specific synapse rather than random or equal distribution as indicated by our AVD and AVA measurements (Figure 2G). The simplest interpretation is that there are postsynaptic changes in the downstream neurons.

Loss of synchrony is reversible and can be separated from magnitude of calcium increase in the ASH

Delayed response could also be a way for the circuit to function in all states (both awake and lethargus) when calcium activity in the ASH in decreased. In fact, decreased avoidance response to ASH-specific stimuli has been attributed to decreasing calcium activity in dopamine-treated animals (Ezcurra et al., 2011). Although neuromodulator-mediated sensory dampening is seen as decreases in behavioral response in the presence of serotonin or dopamine (Ezcurra et al., 2011), reversibility in behavior is more specific to the sleep state.

Furthermore, the source of reversibility is unknown. To analyze the cause of dynamics of reversibility, we need to know whether it is the magnitude of calcium increase at a sensory neuron or the response of downstream components that is reversible.

Therefore, we measured lethargus animals expressing GCaMP in ASH, AVD, and AVA in the microfluidic chip with and without a mechanical stimuli preceding glycerol stimulation. Individual animals showed the same trend: calcium increase in the ASH did not differ significantly between unperturbed and perturbed trials (Figure 3A–B), but the activity in the downstream interneurons was both coordinated and immediate in trials following mechanical stimulation (Figure 3A). This result indicates that although varying presynaptic input from the ASH may change circuit function and behavior, there are other postsynaptic factors that modulate transmission at these synapses. Furthermore, these changes are dependent upon previous stimulation at the level of the interneurons.

Modulation in lethargus also lies downstream of ASH depolarization

We validated imaging data and assessed the contribution of downstream neurons to lethargus behavior using the genetically encoded light-activated cation channel Channelrhodopsin2 (ChR2). In the presence of its cofactor, all-trans retinal (ATR), ChR2 allows control of both the extent and timing of cellular depolarization through optical stimulation (Lindsay et al., 2011; Narayan et al., 2011; Zhang et al., 2007). Changes in the sensory response to ASH-mediated noxious stimuli (such as copper or glycerol) is modulated by the presence food or exogenous application of dopamine, but these responses are modality-specific and are absent in response to mechanical stimuli (Ezcurra et al., 2011). Optogenetic activation of ASH was shown to be unaffected by changing conditions (Ezcurra et al., 2011). Direct control of ion channels and normalization of the initial current injection allows for better assessment of the downstream components of the avoidance circuit by bypassing ligand-binding and associated membrane depolarization in ASH.

Neurons classes in each level of the avoidance circuit were individually depolarized. We used animals in which ChR2 is expressed exclusively in the ASH (Ezcurra et al., 2011), and found that light-driven activation induced robust and active reversal behavior in both the L4 and young adult animals (Figure 4B). However, behavioral response delay persists upon ChR2-mediated ASH depolarization during lethargus: the average time to respond to the ChR2 stimulation increased from 2s to 18s in lethargus (Figure 4B). Therefore, behavioral delay is not likely due to the decrease in receptor associated depolarization at the ASH, is different from dopamine-mediated modulation, and suggests the existence of additional modulation in downstream components of the circuit. This conclusion is further supported by our finding that regional stimulation ChR2 in the ASH dendrite using targeted illumination can in fact induce calcium increase as measured by GCaMP3 in and out of lethargus (Figure S3E).

Activation of multiple command interneurons is sufficient to induce awake-like behavior

We next activated the downstream command interneurons using the *nmr-1* transcriptional control region to drive ChR2 in AVA, AVD, and AVE (Figure S4A). AVA activity promotes avoidance behavior (Chalfie et al., 1985), and upon direct depolarization of the reverse command interneurons, animals both in and out of lethargus responded immediately (Figure 4C). We further tested activation of AVA alone by targeted illumination of the AVA in animals expressing ChR2 in AVA and RIG. RIG is an interneuron that does not induce changes in locomotion upon activation by ChR2 (Schmitt et al., 2012). Activation of ChR2 in this line with whole body or targeted illumination of AVA alone induces robust reversal in adult worms (Schmitt et al., 2012), but fails to do so consistently or quickly in lethargus (Figure 4D, Figure S5E–G; Movies S1, S2). We used a strain expressing ChR2 in AVA and

RIG for AVA targeted illumination experiments because the AVA is anatomically more distant from the RIG as compared to the command interneurons or the RIM. However, we also tested the AVA with RIM and found similar results to that seen in AVA and RIG (Figure S5F). Thus, if and when interneurons are activated together, a rapid behavioral response followed. The lack of a rapid response upon direct ASH depolarization indicates that transmission of excitatory information from the sensory to the interneurons is decreased or delayed in lethargus.

It is conceivable that that the inability of AVA activation to generate immediate reversal during lethargus may be due to decreasing ChR2 expression in AVA. Therefore, we measured the expression level of ChR2 in the AVA and found that it did not change significantly in and out of lethargus (Figure S4B,D). Lack of altered expression suggests that AVA alone is not sufficient to trigger robust reversals during lethargus. Multiple interneuron input is a crucial component for consistent generation of immediate reversals.

Direct activation of the cholinergic motor neurons including the VA reverse motor neurons showed no significant response latency between the response of L4, lethargus, and young adulthood (Figure 4F), suggesting that the modulation of signaling during lethargus did not occur downstream of the AVA interneuron and remained consistent with previous data indicating that the amount of contraction did not change in lethargus (Dabbish and Raizen, 2011). The importance of synchronous activity in multiple neurons reflects the signal amplification that occurs in the circuit to promote reversal. Amplification can occur through two not necessarily distinct mechanisms: excitation of multiple interneurons by ASH and further amplification of that signal by multiple feed forward loops in the circuit (Figure 4A).

Increasing the extent of ASH but not AVA depolarization can elicit immediate response

Previously published work describes the avoidance circuit as a coherent type 1 feed forward loop, the dynamics of which have been modeled (Figure S5A) (Kashtan et al., 2004). This circuit motif creates delay by preventing processing in the AVA until both ASH and AVD are active (Kashtan et al., 2004). Our simulation of dynamics using the published model show that adjusting the threshold or ratio of transfer at the ASH to interneuron synapses (even in the absence of input change) can cause a delay, which can be shortened by increasing activity at the ASH (Figures S5B). We therefore stimulated ChR2-expressing ASH neurons in a graded manner. To more strongly activate ASH, we used a 100-fold higher concentration of ATR and a 2.5-fold stronger light intensity. When subjected to this stronger stimulus, animals in lethargus displayed a reduced behavioral delay not significantly different from that of young adults (Figures 5C; S6A–B). These results are consistent with the model and suggest either the threshold or transfer at the synapse changes during lethargus, requiring significantly more presynaptic depolarization to elicit an immediate response. Increasing ASH input should increase activity at the AVD as well as the AVA, implying that the increased input to motor neurons may no longer be linear and is possibly exponential. Increased current injection at RIM and AVA does not suppress response delay (Figure 5E), raising the possibility that a single command interneuron may not be able to output sufficient signal to the motor neurons to generate immediate response and that synchronous activation of the command interneurons is likely necessary for rapid reversal.

Response delay to ASH depolarization is reversible upon previous stimulation

To further understand the decreased transmission between sensory and inter-neurons during lethargus, we stimulated interneurons through an ASH-independent circuit (Figure 5A). Mechanosensation at the body wall promotes reversal by activating the AVA and AVD command interneurons independent of ASH (Chatzigeorgiou and Schafer, 2011; Li et al.,

2011). FLP, a mechanosensory neuron, responds to harsh touch to the anterior body (Chatzigeorgiou and Schafer, 2011). When animals are woken by a harsh touch, they reverse immediately. After a full reversal, animals are more responsive to ChR2 stimulation, and the average response delay to ChR2-induced ASH depolarization is 2s, suppressing the response delay normally seen in lethargus (Figure 5B). Surprisingly, promoting forward locomotion using PLM/PVM-mediated tail touch, which functionally should inhibit AVD and AVA, also suppressed response delay (Figure 5B). It is thus not important whether the animals are moving forward or backward, but that they are active. Waking the animal during lethargus does not suppress response delay to AVA depolarization (Figure 5D), indicating that input into multiple command neurons is required. These results suggest that there is an awake state that determines the interneuron resistance to signal processing, and waking primes the interneurons to respond to sensory stimuli.

Circuit modulations seen in lethargus are general and dependent on arousal state

Behavioral quiescence can be observed outside of lethargus and in the adult stage during satiety behavior (You et al., 2008) and during EGF-overexpression (Van Buskirk and Sternberg, 2007). Satiety can be induced with high nutrient food and is enhanced when a long period of starvation is followed with food (You et al., 2008). We examined the behavior of animals three hours after refeeding and observed quiescence, as measured by pharyngeal pumping and locomotion (Figure 6A–B). Animals that were fasted and refed showed delayed response to ASH activation with ChR2 when compared with starved or continuously fed animals (Figure 6C). Moreover, this delay was reversible and was suppressed by previous mechanical stimulation (Figure 6D). These results show that sleep-like behavior is not restricted to lethargus and suggest the changes in the avoidance circuit is not tied to the developmental stage but physiological state of the animal.

EGF overexpression in young adult animals showed similar results. EGF signalling was implicated as a quiescence promoting component during lethargus, and anachronistic expression strongly induces quiescence (Van Buskirk and Sternberg, 2007). Therefore, we induced quiescence by overexpressing EGF in young adult animals (Figure 6E) and found that animals had a delayed response to ASH activation comparable to lethargus (Figure 6F). Also, delayed response due to EGF could also be reversed upon previous stimulation by a tail tap (Figure 6G). These results show that sleep-like behavior induced outside of lethargus by satiety and one component of lethargus signalling is effective in replicating the behavioral dynamics.

In addition, we found that rebound homeostatic behavior seen following disruption of lethargus (Raizen et al., 2008) can be seen in response to ChR2 activation (Figure S6E). These data suggest that lethargus occurs by downstream circuit modulation, and can be driven and adjusted by previous activity and by environmental factors. Furthermore, these observations eliminate the possibility of developmental factors being the primary driver of neuronal modulation.

We also tested whether the observed sensory neuron modulation is restricted to ASH or to circuits mediating avoidance. We chose to study the gustastatory neuron, ASE, during and out of lethargus. Unlike ASH, ASE senses attractive stimuli, like preferred salt concentration, has no mechanical component, and promotes forward locomotion. We found that ASE also shows decreased calcium transients during lethargus (Figure S6F), implying that circuit modulations are likely general across the sensory layer and similar modulation likely exist in the forward command interneurons.

Discussion

We examined the well-characterized ASH avoidance circuit during sleep and waking and found that decreased arousal during sleep stems from not only the worm's inability to robustly sense the incoming stimulus but also a failure to activate components of the circuit that promote avoidance in the awake state. We found significant modulation in both sensory and command interneuron activity during lethargus and confirmed the function of observed activity patterns using channelrhopdopsin to optically control activity in single or select groups of neurons. We also find that dampened sensory activity in the ASH neuron is likely correlated with the presence of sleep drivers, is constant during lethargus, and is minimally altered in response to optogenetic stimuli after mechanical stimulation preceeding the measured trial duration. This neuronal activity is in stark constrast to the dynamics of behavior: sensory response to ASH activation by chemical stimuli is immediate upon previous waking with mechanical stimuli. However, changes in dynamics are well correlated with coordinated activity of the command interneurons AVD and AVA. Moreover, this coordinated activity that is lost during quiescence is recovered upon waking.

How might activation of interneurons by one sensory neuron sensitize them to other sensory neurons? One mechanism of decreasing threshold is to make the interneuron more receptive to presynaptic input by activity-driven changes in receptor localization (Metherate, 2004; Metherate and Hsieh, 2004). In addition, activity-driven changes in synaptic tranmission and transfer can be readily explained by disinhibition (Letzkus et al., 2011) or neurotransmitter availability. The fast dynamics of reversibility during sleep make it unlikely that neuromodulators are directly responsible for the reversibility because unbinding from targets and breakdown or sequestration of peptides would not be possible in the time scale of behavioral dynamics (milliseconds to seconds). In addition, the mediation of reversible transmission by a secondary intermediate outside of the sensory motor circuit is precluded by the lack of candidates with the proper connectivity to all sensory neurons or even the sensory neurons published or tested in this work (White et al., 1986).

Both decreased sensory transduction and reversible resistance in transmission of excitatory information downstream occurs, and the presence of these modulations pose interesting questions about the utility of having multiple levels of modulation. Decreasing the magnitude of ASH response results in decreased signal processed downstream, and theoretically, in a smaller probability of reaching threshold to relay information to downstream components of the circuit (Figures S3B, S4A). This type of sensory gating would help prolong inactivity in the sensory motor circuit and promote behavioral quiescence. However, direct alteration of the response of individual sensory neurons after waking or even all sensory neurons after waking would perpetuate a long awake state because the nervous system would not be sufficiently gated, and this might continue reponding to basal sensory stimuli as well as mechanical stimuli from locomotion. Thus, if sleep and wakefulness in the worm are regulated only by gating and lack of gating, respectively, at the sensory neuron, then the dynamics in the circuit create a positive feedback loop because activity in the circuit would sensitize the sensory neuron and promote more activity in the circuit, and so on. Furthermore, constant decrease in ASH activity makes the circuit more sensitive to small changes in signal transduction or synaptic tranmission to AVA and AVD, lengthening the range of behavioral delay and decreasing the probability of downstream synchronization (Figure S3A–B). Dynamic sensitization of the command interneurons allows for increased probability of coordinated activity upon previous stimulation, but requires sensory input to multiple command neurons (Figure 7). Therefore, the use of coordinated activity in downstream components offers flexibility and fast behavioral dynamics while simultaneously ensuring that waking leads to sensitivity to all modalities as well as sensory neurons that converge upon the command neurons.

We found that behavioral delay and reversibility is not exclusively limited to lethargus: they occur with EGF expression and with quiescence induced by satiety, indicating that these circuit modulations are due to behavioral state and not developmental stage. Thus, these results are more relevant to understanding behavioral states across species. Also, sensory dampening is likely general in sensory motor circuits, and sensory neurons associated with food and attractive stimuli are dampened in addition to those for pain and noxious stimuli.

Past circuit understanding of sleep is limited to a general understanding of loss of synchrony between cortex and thalamus due to inability of the thalamus to relay information to the cortex (Jones, 2009; Magnin et al., 2010). We have demonstrated similar changes of information relay from sensory to command interneurons in a simple circuit of *C. elegans*. Decrease in sensory signaling contributes to, but is not the sole factor of, changing information relay. Excitability of the downstream command interneurons is also likely altered and serves as a point for reversible function of the circuit during the sleep-like state. Thus, small changes in dynamics at multiple levels promote and prolong quiescence while allowing reversibility of behavior upon sufficient stimulus by using components of a circuit that appear redundant, but serve to amplify or suppress input signal. The *C. elegans* nervous system is condensed when compared to a mammalian nervous system. We can then conjecture that a sensory neuron in the worm may serve to perform both sensory functions and the processing that presumably occur downstream in other less compact neural circuits. Regardless, these components of multilevel modulation serve as one strategy for generating the dynamic behaviors seen in sleep.

Experimental Procedures

Strains

Caenorhabditis elegans strains were maintained under standard conditions at 20°C (Brenner 1974). The following strains were used in this study:

ASH ChR2: AQ2235 *lite-1(ce314); ljIs114[Pgpa-13::FLPase; Psra-6::FTF::ChR2::YFP]* (Ezcurra et al., 2011),

AVA, RIM ChR2: ZX1038 *lin-15(n765ts); lite-1(ce314); zxEx704[pflp18::loxP::LacZ::STOP::loxP:: ChR2::mCherry::SL2::GFP* (80 ng/μl); *pgpa-14::Cre* (80 ng/μl); *lin-15+]* (Schmitt et al., 2012),

AVA, RIG ChR2: ZX1020 *lin-15(n765ts); zxEx717[pflp18::FRT::mCherry::STOP::FRT:: ChR2::YFP* (80 ng/μl); *prig-3::FLP* (80 ng/μl); *lin-15+]* (Schmitt et al., 2012)

Cholinergic motor neuron ChR2: EG5096 [*Punc-17:ChR2::mCherry*] (Dabbish and Raizen, 2011),

ASH ChR2 with ASH, AVD, and AVA GCaMP3: SRS85 *sraIs49 [nmr-1p::G-CaMP; unc-119(+)]; lite-1(ce314); sraEx80 [sra-6p::chop-2(H134R)::mCherry; osm-10p::G-CaMP; unc-122p::mCherry]* (Guo et al., 2009),

AVA cameleon: PS5955 (*Prig-3:: cameleon*),

ASH cameleon: *ljEx95[Psra-6::YC2.12]*(Hilliard et al., 2005).

Molecular biology

The genetically encoded light-activated channelrhodopsin gene *ChR2* (a gift from the Deisseroth lab) was cloned into the pPD96.52 Fire vector (Addgene) to generate a *ChR2::YFP* fusion with the *unc-54 3′utr*. This construct was fused to a 5 kb sequence from

upstream of the *nmr-1* gene previously demonstrated to drive expression in AVA and AVD. Expression was confirmed in AVA, AVD, and AVD interneurons (Guo et al., 2009).

Chip Fabrication

We designed chips in AutoCAD (Autodesk) and sent the design to a mask-making service (Photosciences), which provided the chrome masks. We created the master molds by spin casting at 3,000 r.p.m and patterning a 19-μm-thick layer of SU-8 photoresist (MicroChem) on bare silicon wafers. We used previously published procedures to prepare the master molds for use with polydimethylsiloxane (PDMS) and perform the soft lithography to make the PDMS replicas (Park et al., 2006). The PDMS replicas were treated with air plasma (40W for 12s) to activate the PDMS surface and manually bond it to a coverslip. The chips were ethanol treated and flushed with FU-18 before use.

Calcium imaging

Calcium imaging was performed in a microfluidic device essentially as described (Chronis et al., 2007). The device was altered in only the part of the chip that constrains the worm ro fit different developmental stages. Several versions were made in which the dimensions were scaled to fit an animal 600μm in length and 30–60μm in diameter. The flow of stimuli and buffers in the device was controlled using an external valve system to regulate pressure at the various inlets, which modified the pattern of flow. External components were built according to published protocols to automate the valve system (Rafael Góez-Sjöerg, Microfluidics Lab, Lawrence Berkeley National Laboratory), and valves were controlled using LabView software (National Instruments). Fluorescence time-lapse imaging (100-ms exposures, 5Hz) was performed on a Zeiss Axioscope inverted microscope with a 40x air objective and an Andor EMCCD camera. Animals were presented with alternating streams of S-basal complete buffer and stimulant (Cu2+ or glycerol) in S-complete buffer. All image analysis was done using a custom script written in Matlab: after background subtraction, total fluorescence intensity was measured from the individual regions of interest (ROIs) corresponding to the cell body. No adjustments were done for photobleaching as there was minimal evidence of such with the low intensity light exposure.

Analysis of Calcium Events

Exponential smoothing of the calcium imaging data was performed in Matlab (alpha value of 0.05) and instantaneous time derivatives were calculated for each time point. These values were plotted in a raster plot (Figures 2C, S3C) and were characterized as a calcium increase (>0) or decrease (<0). These events were further binned into 1s bins to quantify the probability of these events during the duration of the imaging and response to buffer or glycerol. Cross correlation was performed on the data of corresponding ASH-AVD, ASH-AVA, and AVD-AVA traces. The value at lag time=0 or peak correlation was used to assess differences between different neuron sets and conditions.

Behavior

Unless otherwise stated, AQ2235 animals were grown in the dark with 10μM ATR and were illuminated with blue light (425–475 nm) from an LED device (Phillips LumiLEDS) at 12mW intensity at the level of the plate. EG5096 and ZX1020 animals were grown in the dark with 100μM ATR, picked onto a new ATR plate, allowed to rest for 10 minutes, and were illuminated with blue light (425–475 nm) from an LED device (Phillips LumiLEDS) at 12mW and 30mW intensity at the level of the plate. Animals were stimulated with an LED device when stationary or exhibiting forward locomotion, and imaged during the assay for behavioral analysis using a Leica stereomicroscope and a Unibrain camera using Unibrain software. Reversal was scored as posteriorwards movement that was greater than the length

of the worm's head. Three trials were performed for each worm, and the interval between trials was 30 seconds.

Worms were perturbed for the waking assays by harsh touch with a worm pick immediately anterior to the middle of the worm (marked by the vulva) or by tail touch with an eyelash drawn across the tail of the worm. ChR2 assays were performed when the animals exhibited stationary behavior or forward locomotion (all stimulations were performed within 30s of the perturbation).

Worms that were tested for lethargus homeostasis by 30-minute perturbation in lethargus or L4 stage were stimulated by tail touch with an eyelash drawn across the tail of the worm every minute or when the worm was observed to be quiescent (whichever came first). ChR2 assays were performed when the animals exhibited stationary behavior for the baseline measurement. Then, animals were again perturbed with tail touch and tested immediately after as well as 2 minutes, 5 minutes, and 30 minutes after the tap.

Targeted illumination

All targeted illuminations were performed with Leica model DMI600 and Mosaic 2 (Andor Technologies). For behavior experiments low intensity halogen light was used to visualize the worm while the Mosaic micromirror array targets individual neurons with blue light (450–480 nm) from an LED light source (XLED, Lumen Dynamics). For GCaMP3 measurements, the whole field of view was illuminated with blue light (450–480 nm) from the XLED, that was further attenuated with an external 435–470nm optical filter while the Mosaic micromirror array targets individual neurons with higher intensity blue light (450–480 nm).

Modeling

All simulations were performed using custom scripts in Matlab with parameters and equations previously published (Kashtan et al., 2004). Individual variables (e.g. ASH activity), were generated by allowing the script to generate values at the various input values where other variables (ASH threshold, AVD threshold, AVA threshold) were fixed. The script ran variations of different combinations to generate the data plotted in the activity vs. time plots shown in Figures S7B.

Supplementary Material

Refer to Web version on PubMed Central for supplementary material.

Acknowledgments

References

Allada R, Siegel JM. Unearthing the phylogenetic roots of sleep. Curr Biol. 2008; 18:R670–R679. [PubMed: 18682212]

Bargmann, CI. WormBook : the online review of C elegans biology. 2006. Chemosensation in C. elegans; p. 1-29.

Ben Arous J, Tanizawa Y, Rabinowitch I, Chatenay D, Schafer WR. Automated imaging of neuronal activity in freely behaving Caenorhabditis elegans. J Neurosci Methods. 2010; 187:229–234. [PubMed: 20096306]

Chalfie M, Sulston JE, White JG, Southgate E, Thomson JN, Brenner S. The neural circuit for touch sensitivity in Caenorhabditis elegans. J Neurosci. 1985; 5:956–964. [PubMed: 3981252]

Chatzigeorgiou M, Schafer WR. Lateral facilitation between primary mechanosensory neurons controls nose touch perception in C. elegans. Neuron. 2011; 70:299–309. [PubMed: 21521615]

Chronis N, Zimmer M, Bargmann CI. Microfluidics for in vivo imaging of neuronal and behavioral activity in Caenorhabditis elegans. Nat Methods. 2007; 4:727–731. [PubMed: 17704783]

Dabbish NS, Raizen DM. GABAergic synaptic plasticity during a developmentally regulated sleep-like state in C. elegans. J Neurosci. 2011; 31:15932–15943. [PubMed: 22049436]

Ezcurra M, Tanizawa Y, Swoboda P, Schafer WR. Food sensitizes C. elegans avoidance behaviours through acute dopamine signalling. EMBO J. 2011; 30:1110–1122. [PubMed: 21304491]

Foltenyi K, Greenspan RJ, Newport JW. Activation of EGFR and ERK by rhomboid signaling regulates the consolidation and maintenance of sleep in Drosophila. Nat Neurosci. 2007; 10:1160–1167. [PubMed: 17694052]

Guo ZV, Hart AC, Ramanathan S. Optical interrogation of neural circuits in Caenorhabditis elegans. Nat Methods. 2009; 6:891–896. [PubMed: 19898486]

Hilliard MA, Apicella AJ, Kerr R, Suzuki H, Bazzicalupo P, Schafer WR. In vivo imaging of C. elegans ASH neurons: cellular response and adaptation to chemical repellents. EMBO J. 2005; 24:63–72. [PubMed: 15577941]

Hilliard MA, Bargmann CI, Bazzicalupo P. C. elegans responds to chemical repellents by integrating sensory inputs from the head and the tail. Curr Biol. 2002; 12:730–734. [PubMed: 12007416]

Jones EG. Synchrony in the interconnected circuitry of the thalamus and cerebral cortex. Annals of the New York Academy of Sciences. 2009; 1157:10–23. [PubMed: 19351352]

Kashtan N, Itzkovitz S, Milo R, Alon U. Topological generalizations of network motifs. Physical review E, Statistical, nonlinear, and soft matter physics. 2004; 70:031909.

Letzkus JJ, Wolff SB, Meyer EM, Tovote P, Courtin J, Herry C, Luthi A. A disinhibitory microcircuit for associative fear learning in the auditory cortex. Nature. 2011; 480:331–335. [PubMed: 22158104]

Li W, Kang L, Piggott BJ, Feng Z, Xu XZ. The neural circuits and sensory channels mediating harsh touch sensation in Caenorhabditis elegans. Nature communications. 2011; 2:315.

Lindsay TH, Thiele TR, Lockery SR. Optogenetic analysis of synaptic transmission in the central nervous system of the nematode Caenorhabditis elegans. Nature communications. 2011; 2:306.

Magnin M, Rey M, Bastuji H, Guillemant P, Mauguiere F, Garcia-Larrea L. Thalamic deactivation at sleep onset precedes that of the cerebral cortex in humans. Proc Natl Acad Sci U S A. 2010; 107:3829–3833. [PubMed: 20142493]

Metherate R. Nicotinic acetylcholine receptors in sensory cortex. Learn Mem. 2004; 11:50–59. [PubMed: 14747517]

Metherate R, Hsieh CY. Synaptic mechanisms and cholinergic regulation in auditory cortex. Prog Brain Res. 2004; 145:143–156. [PubMed: 14650913]

Monsalve GC, Van Buskirk C, Frand AR. LIN-42/PERIOD controls cyclical and developmental progression of C. elegans molts. Curr Biol. 2011; 21:2033–2045. [PubMed: 22137474]

Narayan A, Laurent G, Sternberg PW. Transfer characteristics of a thermosensory synapse in Caenorhabditis elegans. Proc Natl Acad Sci U S A. 2011; 108:9667–9672. [PubMed: 21606366]

Park JW, Vahidi B, Taylor AM, Rhee SW, Jeon NL. Microfluidic culture platform for neuroscience research. Nat Protoc. 2006; 1:2128–2136. [PubMed: 17487204]

Piggott BJ, Liu J, Feng Z, Wescott SA, Xu XZ. The neural circuits and synaptic mechanisms underlying motor initiation in C. elegans. Cell. 2011; 147:922–933. [PubMed: 22078887]

Raizen DM, Zimmerman JE, Maycock MH, Ta UD, You YJ, Sundaram MV, Pack AI. Lethargus is a Caenorhabditis elegans sleep-like state. Nature. 2008; 451:569–572. [PubMed: 18185515]

Schmitt C, Schultheis C, Husson SJ, Liewald JF, Gottschalk A. Specific expression of channelrhodopsin-2 in single neurons of Caenorhabditis elegans. PLoS One. 2012; 7:e43164. [PubMed: 22952643]

Schwarz J, Lewandrowski I, Bringmann H. Reduced activity of a sensory neuron during a sleep-like state in Caenorhabditis elegans. Curr Biol. 2011; 21:R983–984. [PubMed: 22192827]

Siegel JM. The REM sleep-memory consolidation hypothesis. Science. 2001; 294:1058–1063. [PubMed: 11691984]

Van Buskirk C, Sternberg PW. Epidermal growth factor signaling induces behavioral quiescence in Caenorhabditis elegans. Nat Neurosci. 2007; 10:1300–1307. [PubMed: 17891142]

Ward S, Thomson N, White JG, Brenner S. Electron microscopical reconstruction of the anterior sensory anatomy of the nematode Caenorhabditis elegans.?2UU. J Comp Neurol. 1975; 160:313–337. [PubMed: 1112927]

White JG, Southgate E, Thomson JN, Brenner S. The structure of the nervous system of the nematode Caenorhabditis elegans. Philosophical transactions of the Royal Society of London Series B, Biological sciences. 1986; 314:1–340.

Yizhar O, Fenno LE, Davidson TJ, Mogri M, Deisseroth K. Optogenetics in neural systems. Neuron. 2011; 71:9–34. [PubMed: 21745635]

You YJ, Kim J, Raizen DM, Avery L. Insulin, cGMP, and TGF-beta signals regulate food intake and quiescence in C. elegans: a model for satiety. Cell Metab. 2008; 7:249–257. [PubMed: 18316030]

Zhang F, Wang LP, Brauner M, Liewald JF, Kay K, Watzke N, Wood PG, Bamberg E, Nagel G, Gottschalk A, et al. Multimodal fast optical interrogation of neural circuitry. Nature. 2007; 446:633–639. [PubMed: 17410168]

Zimmerman JE, Naidoo N, Raizen DM, Pack AI. Conservation of sleep: insights from non-mammalian model systems. Trends Neurosci. 2008; 31:371–376. [PubMed: 18538867]

Highlights

- Multiple sensory neurons are dampened during sleep

- Coordinated interneuron activity is suppressed in sleep and recovered upon waking

- Reversibility of sleep is regulated by activity at the command interneuron level
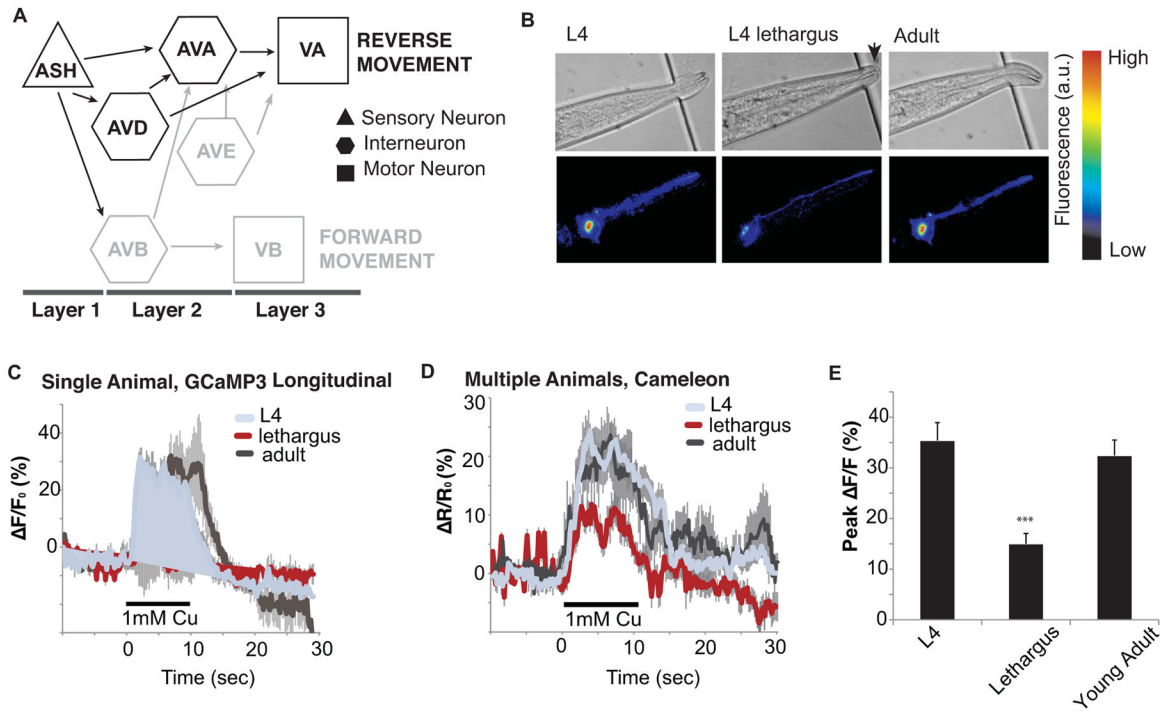
- Similar circuit changes occur in three types of sleep

Figure 1. Sensory depression occurs in the ASH polymodal sensory neuron
(A) Functional model of the avoidance circuit. The two polymodal ASH sensory neurons work through the two AVA and two AVD interneurons to promote reversal through the VA motorneurons. Neurons tested in the study are darkened. **(B)** Single frames of GCaMP3 DIC and fluorescence recording in ASH over the L4, lethargus, and young adult stages. Arrow denotes the cuticle cap that marks lethargus. **(C)** Representative GCaMP3 traces of a single worm as it transitions from L4 to lethargus to young adult. **(D)** Average change in cameleon fluorescence in the ASH sensory neuron over time in a short calcium imaging assay. L4 and lethargus response to 1mM Cu^{2+} (L4 n=10; L4 lethargus n=11). **(E)** The calcium increase in response to 1mM Cu2+ is significantly decreased in lethargus (n=11) as compared to L4 (n=10) and young adult (n=5; ***p<0.001, Student's t-test equal variance). See also Figure S1.
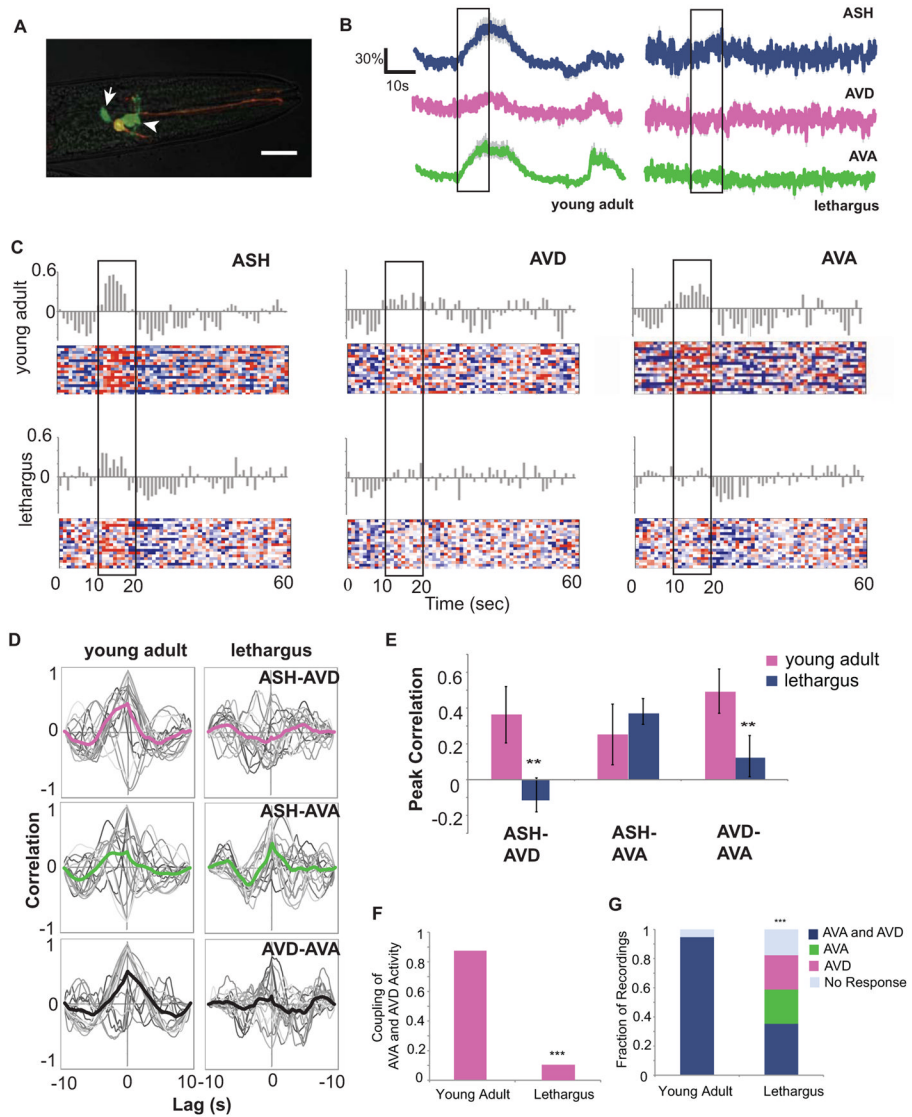
Figure 2. AVD loses synchrony with AVA in lethargus
(A) Image of the neurons in which GCaMP3 was measured. ASH is marked by the presence of both GCaMP3 and mCherry, AVD is posterior (white arrow), and AVA is anterior (white arrowhead). **(B)** Representative traces of a glycerol trial in a single animal in both lethargus and young adult. **(C)** Heat map of 60s trials denoting increase (red) and decrease (blue) in young adult (n=18) and lethargus (n=18). The proportion of increase or decrease were averaged across trials in 1s bins and are denoted by the gray bars above the heat maps. **(D)** Cross correlation of the stimulus interval between ASH-AVD, ASH-AVA, and AVA-AVD. Individual cross correlations are shown as gray lines, the average by the colored line. Correlation of 1 is a perfect match, and correlation of −1 denotes an inverse relationship. AVD exhibits an average lag in response and shows a decreasing correlation with AVA during lethargus. **(E)** Peak correlation values extracted from the cross correlation analysis. AVD loses its synchronicity with ASH and AVD only in lethargus (p<0.01, n=18, students t-test of unequal variance). AVA shows no decrease in correlation with ASH. **(F)** Quantification of trials in which GCaMP3 measurements of AVA and AVD showed corresponding trains of calcium increase during the course of the trial. The majority of trials

in the young adult (0.86, n=23) showed coupled activity, but this coupling decreased significantly in lethargus (p<0.000001, 0.12, n=16). Many of the trials in lethargus showed activity in either AVA or AVD, while young adult animals did not show any instances of this pattern of activity (p<0.0001). See also Figure S2.
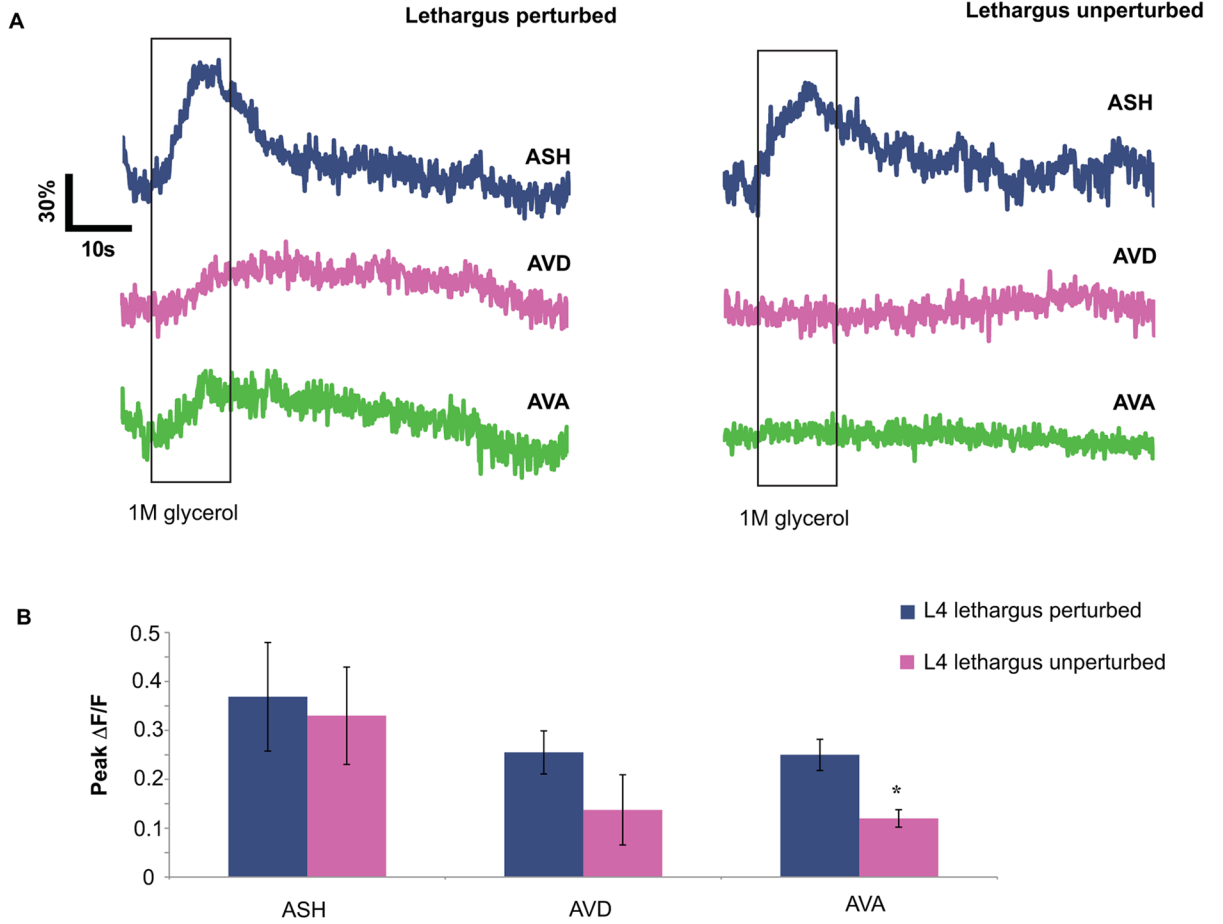
A

Lethargus perturbed

Lethargus unperturbed

30%

10s

ASH

AVD

AVA

1M glycerol

ASH

AVD

AVA

1M glycerol

B

■ L4 lethargus perturbed
■ L4 lethargus unperturbed

Peak ΔF/F

0.5

0.4

0.3

0.2

0.1

0

ASH   AVD   AVA

*

Figure 3. Loss of synchrony is reversible and can be separated from magnitude of calcium increase in the ASH

(A) Representative GCaMP3 measurements of ASH, AVD, and AVA of a single worm in response to 1M glycerol with and without previous mechanical stimulation during lethargus. **(B)** Perturbation does not significantly affect peak increase in ASH as measured by GCaMP3, but it does cause significant increase in responsivity at the AVA (*p<0.01, n=4, students t-test of unequal variance). See also Figure S3.
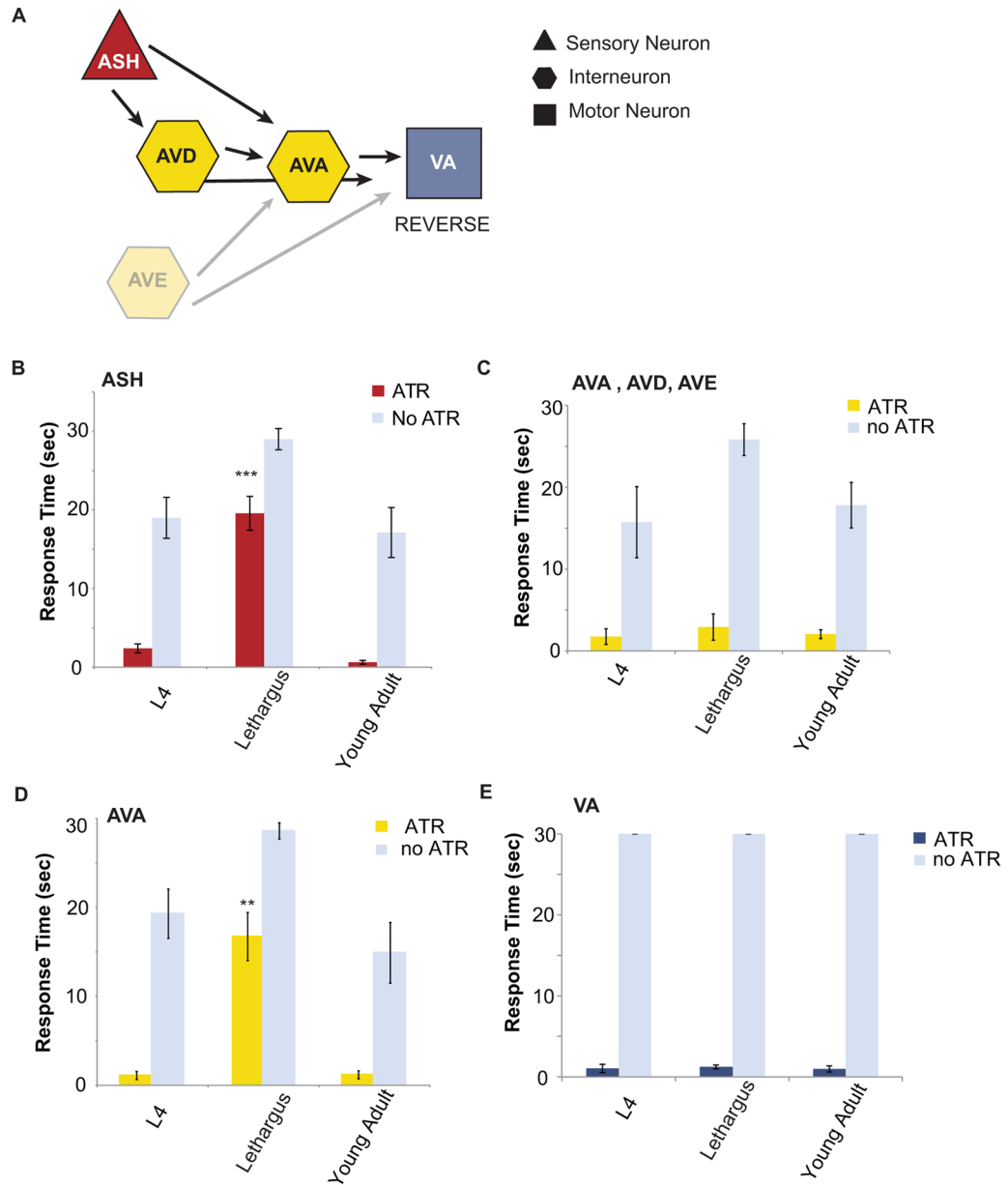
Figure 4. Sensory modulation occurs downstream of ASH depolarization
(A) Schematic diagram of the neurons manipulated to generate reversal. ASH promotes activity at the AVD and AVA interneurons. **(B)** Behavioral response times to ASH depolarization using channelrhodopsin. The mean ± s.e.m. values are shown: L4 (n=13), lethargus (n=9), adult (n=7); ***p=0.0001, ANOVA. All ATR treated animals were compared to their paired non-ATR treated controls L4 (n=13), lethargus (n=9), adult (n=7); p<0.0001, Student's t-test of unequal variance. **(C)** AVA, AVE, and AVD were depolarized using channelrhodopsin. Avoidance behavior did not differ significantly between worms in and out of lethargus. L4 (n=7), lethargus (n=6), adult (n=6); ANOVA. All ATR treated animals were compared to their paired non-ATR treated controls L4 (n=7), lethargus (n=6), adult (n=6); p=<0.0001, Student's t-test equal variance. **(D)** Depolarization of AVA without the other command interneurons showed a significant delay in lethargus (n=13) when compared with L4 (n=7) and adult (n=6); **p<0.001, ANOVA. All ATR treated animals

were compared to their paired non-ATR treated controls L4 (n=6), lethargus (n=10), adult (n=6); p<0.0001, Student's t-test of unequal variance. **(E)** Depolarization of cholinergic motorneurons with channelrhodopsin. L4 (n=5), lethargus (n=5), adult (n=5), ANOVA. All ATR treated animals were compared to their paired non-ATR treated controls L4 (n=13), lethargus (n=9), adult (n=7); ***p<0.0001, Student's t-test equal variance. See also Figure S4.
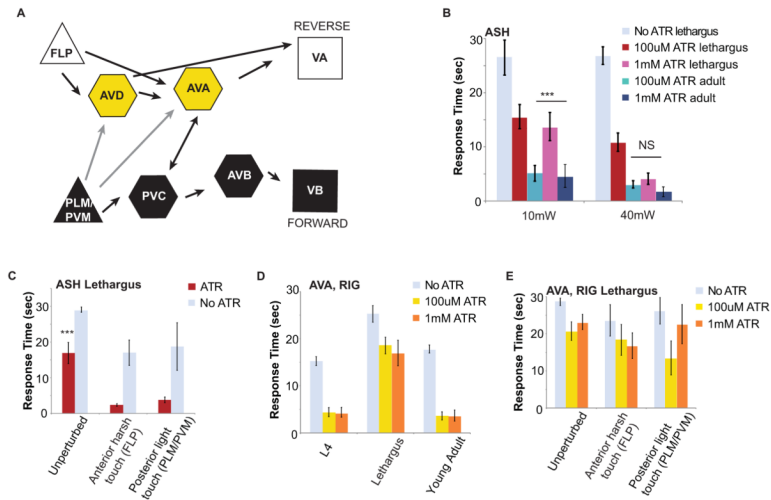
Figure 5. Reversibility arises from interneuron activation but requires simultaneous input to both AVD and AVA

(A) Schematic diagram of the neurons manipulated to generate reverse locomotion. Multiple sensory cues and neurons can induce reversal, including ASH, and FLP (Chatzigeorgiou and Schafer, 2011; Hilliard et al., 2002). FLP neurons are activated in response to harsh mechanical stimulation at the body wall and act independently of ASH to promote activity at the AVD and AVA interneurons. The PLM and PVM mechanosensory neurons work through the PVC interneuron but are also synaptically connected with the AVA and AVD to generate forward locomotion in response to tail touch. **(B)** Behavioral response to 10mW and 40mW of optical stimulation of ChR2 in lethargus and young adult animals at 100μM and 1mM ATR concentrations. **(C)** ASH of lethargus animals were depolarized with ChR2 unperturbed (n=21), after harsh touch at the body wall (n=9), and after tail touch (n=12). Both perturbations suppressed the delay in reversal; ***$p<0.0001$, ANOVA. All ATR treated animals were compared to their paired non-ATR treated controls unperturbed (n=21), after harsh touch at the body wall (n=9), and after tail touch (n=12); $p=<0.0001$, Student's t-test of unequal variance. **(D)** AVA of lethargus animals grown in 0, 100μM, or 1mM ATR were depolarized with ChR2 unpertubed (n=23), after harsh touch (n=10), and after tail touch (n=13). No significant difference was seen between animals grown on 100μM and 1mM ATR. All ATR treated animals were compared to their paired non-ATR treated controls unperturbed (n=23 after harsh touch at the body wall (n=10), and after tail touch (n=13)); $p=<0.0001$, Student's t-test of unequal variance. **(E)** Even with increased ATR concentraion at 1mM, depolarization of AVA in animals continued to show a significant delay in lethargus (n=11) when compared with L4 (n=13) and adult (n=9); ***$p<0.0001$, ANOVA. No significant difference was seen between animals grown on 100μM and 1mM ATR. See also Figure S5.
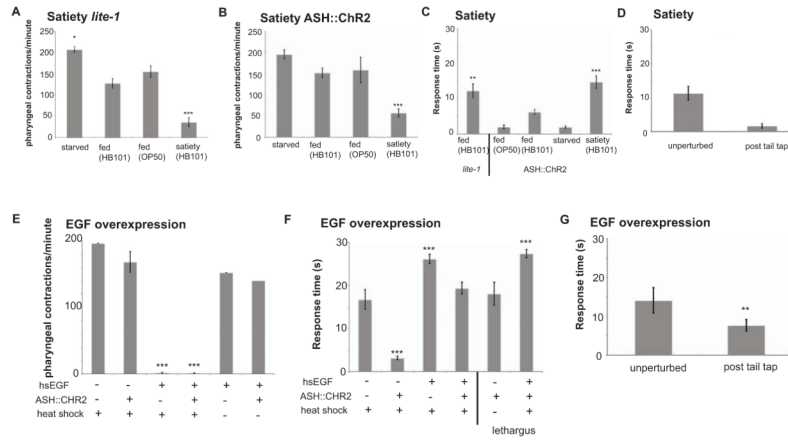
Figure 6. Circuit modulations in lethargus are dependent on arousal state

(A) Feeding activity of *lite-1* animals (which has decreased response to blue light) as indicated by pharyngeal contractions in response to starvation (n=8), feeding on OP-50 (n=9), feeding on HB101 (n=5), and feeding after 12 hours of starvation, i.e. satiety assay (n=14). The mean ± s.e.m. values are shown, *p=0.01, ***p=0.0001, ANOVA. **(B)** Feeding activity of ASH::ChR2 animals as indicated by pharyngeal contractions in response to starvation (n=8), feeding on OP-50 (n=5), feeding on HB101 (n=13), and feeding after 12 hours of starvation, i.e. satiety assay (n=17). The mean ± s.e.m. values are shown, ***p=0.0001, ANOVA. **(C)** Reversal following light activation of *lite-1* (n=8), ASH::ChR2 animals that were subjected to starvation (n=20), feeding on OP-50 (n=13), feeding on HB101 (n=8), and feeding after 12 hours of starvation, i.e. satiety assay (n=17). The mean ± s.e.m. values are shown, **p=0.001, ***p=0.0001, ANOVA. **(D)** Reversal following light activation of ASH::ChR2 animals following the satiety assay before perturbation (n=11) and after tail tap (n=11), ***p=0.0001, Student's t-test of unequal variance. **(E)** Feeding activity as indicated by pharyngeal contractions were measured to assess activity levels of the animals following EGF overexpression by heat shock. Only animals with the heat shock EGF transgene (hsEGF) that were treated with heat shock showed decrease in activity. The mean ± s.e.m. values are shown: heat shock *lite-1* (n=5), heat shock ASH::ChR2 (n=5), heat shock hsEGF (n=11), heat shock hsEGF ASH::ChR2 (n=7), hsEGF (n=5), ASH::ChR2 (n=5), ***p=0.0001, ANOVA. **(F)** Reversal following light activation of heat shocked animals. The mean ± s.e.m. values are shown: heat shock *lite-1* (n=11), heat shock ASH::ChR2 (n=17), heat shock hsEGF (n=18), heat shock hsEGF ASH::ChR2 (n=16), heat shock ASH::ChR2 in lethargus (n=10), heat shock hsEGF ASH::ChR2 in lethargus (n=9), ***p=0.0001, ANOVA. **(G)** Reversal following light activation of hsEGF ASH::ChR2 animals following before perturbation (n=11) and after tail tap (n=11), ***p=0.0001, Student's t-test of unequal variance. See also Figure S6.
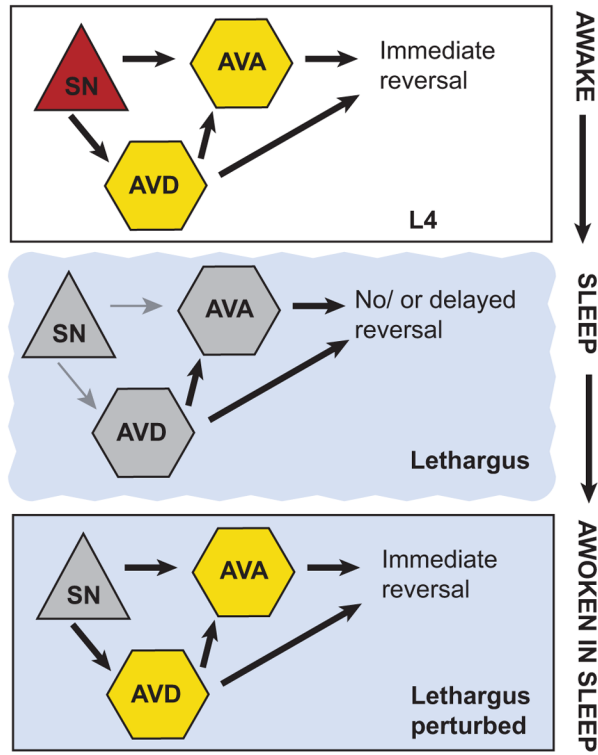
Figure 7. Waking sensitizes the interneurons for coordinated activity
Schematic model of activity in awake animals, during lethargus and waking during lethargus. Greyed neurons indicate modulated function: activity of sensory neuron (SN) in lethargus indicates decreased excitability and the variable timing and dampening of interneuron activity suggest decreased excitability of and/or synaptic transmission of interneurons (AVD and AVA). Arrows mark synaptic connections between the neurons and the gray thin lines denote decrease in transmission across the sensory interneuron synapses during lethargus.